Am J Cancer Res 2023;13(3):872-885
www.ajcr.us /ISSN:2156-6976/ajcr0144880

Original Article

Circ_0000231 promotes paclitaxel resistance in ovarian cancer by regulating miR-140/RAP1B

Jiao Liu[1,2], Han Wang[1], Shuqin Xiao[1], Siyang Zhang[1], Ya Qi[1], Min Wang[1]

[1]Department of Obstetrics and Gynecology, Shengjing Hospital of China Medical University, Shenyang, Liaoning, China; [2]Benxi Central Hospital, Benxi, Liaoning, China

Received June 20, 2022; Accepted January 7, 2023; Epub March 15, 2023; Published March 30, 2023

Abstract: Circular RNAs (circRNAs) are identified as vital regulators in a variety of cancers. However, the involvement of circ_0000231 in paclitaxel (PTX) resistant ovarian cancer (OC) remains unclear. In this study, we examined the levels of circ_0000231, microRNA-140 (miR-140) and RAP1B in PTX-resistant OC tissues and cells and found that circ_0000231 and RAP1B levels were increased, while miR-140 level was decreased in these cells. Depletion of circ_0000231 could inhibit the resistance, proliferation, invasion, migration and EMT and promoted the apoptosis of PTX-resistant OC cells. The opposite effects were observed by overexpression of circ_0000231. Furthermore, the effect of circ_0000231 on the PTX sensitivity of OC cells was investigated by using xenograft tumor models, and circ_0000231 knockdown increased PTX sensitivity of OC in vivo. Mechanistically, we demonstrated that circ_0000231 acted as a sponge for miR-140, and RAP1B was the target gene of miR-140. Taken together, these data indicated that circ_0000231 was a key molecule required for the growth, migration, and PTX-resistance of OC cells and was involved in EMT. Knockdown of circ_000231 suppressed PTX-resistant OC progression via regulating miR-140/RAP1B signaling pathway. circ_0000231 might play vital roles in the tumorigenesis and chemoresistance of OC.

Keywords: Ovarian cancer, circ_0000231, RAP1B, miR-140, chemoresistance, paclitaxel

Introduction

Ovarian cancer (OC) is the eighth most common cause of cancer death and the second cause of gynecologic cancer death in women worldwide [1, 2]. Although PTX-based treatment is one of the first-line chemotherapy regimens, PTX resistance is a major obstacle in this treatment. Different resistance mechanisms have been identified; however, the molecular mechanism of PTX resistance has not been completely elucidated. The development of resistance to chemotherapy in OC patients further complicates OC treatment outcomes [3]. Therefore, understanding the drug resistant mechanism to chemotherapy is critical to improve ovarian cancer treatment efficacy.

Non-coding RNA is a class of RNA transcripts that do not have protein-coding potential, including microRNA (miRNA), long non-coding RNA (lncRNA), and circular RNA (circRNA), which play important roles in the occurrence and development of cancers [4]. CircRNA has become a research focus in the field of non-coding RNA [5]. Several studies have shown that circRNAs can act as a miRNA "sponge" and play an important role in cancer progression [6, 7], especially in drug resistance. For example, circCDR1as inhibits the development of platinum resistance in ovarian cancer by competing with miR-1270 [8]. Furthermore, circCELSR1 acts as a molecular sponge and promotes paclitaxel resistance by competition with miR-1252 for binding to FOXR2 [9]. In addition, circ_0000231 has been reported to attenuate Sevoflurane aroused repression impacts on CRC development by sponging miR-622 [10]. However, the role of circ_0000231 in PTX-resistance in OC remains to be investigated. In this study, we investigated the expression of circ_0000231 in PTX-resistant specimen and cell lines and studied the function as well as the underying potential mechanism of circ_0000231 in OC.

Materials and methods

Specimen collection

The samples from 95 ovarian cancer patients were collected from 2012 to 2019. The diagnosis of all patients was confirmed by surgery and pathology results in the Shengjing Hospital of China Medical University, and all patients only received PTX-based chemotherapy after surgery, the written informed consent form was obtained prior to study initiation from each patient. Patients with primary tumor enlarged or relapsed within 12 months were considered PTX resistance, while other patients were defined as a PTX sensitive. Samples were promptly frozen in liquid nitrogen after surgical dissection and maintained at -80°C deep cryogenic refrigerator until use.

Cell culture

Human ovarian cancer cell line (SKOV3) was purchased from Cell Bank (Shanghai Institute for Biological Science), and PTX-resistant OC line (SKOV3-TR30) was provided by Zhejiang University affiliated Obstetrics and Gynecology Hospital. SKOV3 and SKOV3-TR30 were cultured in RPMI-1640 medium (Solarbio, Beijing, China) supplemented with 10% fetal bovine serum (FBS, Thermo Fisher, Wilmington, DE, USA) and 1% penicillin/streptomycin (Solarbio, Beijing, China) and maintained in a 37°C humidified incubator with 5% CO_2. For SKOV3-TR30 cells, 50 nM PTX was added to the culture medium to maintain PTX resistant phenotype.

RNA extraction and real-time quantitative PCR (qRT-PCR)

Total RNA was isolated from tissues and cells using Trizol (Beyotime, Shanghai, China) according to the manufacturer's protocol. The complementary DNA (cDNA) was obtained using the specific reverse transcription kit (RR047A, Takara, China). Gene expression was determined using SYBR Premix Ex Taq (cat No. RR420A; Takara) and calculated using the 2-ΔΔCt method. The expression of β-actin was used as internal control.

RNase R treatment

For RNase R treatment assay, 10 ug of total RNA was incubated with or without RNase R (Epicentre Technologies, USA) for 30 min at 37°C. Then, the levels of circ_0000231 and linear mRNA (ARHGAP12) were determined by qRT-PCR.

Cell transfection

Small interfering RNAs against circ_0000231 and short hairpin RNA (shRNA) against circ_0000231 (sh-circ_0000231), as well as their corresponding negative controls (si-NC and sh-NC) were synthesized by RiboBio (Guangzhou, China). MiR-140 mimic (miR-140) and its control (miR-NC), and miR-140 inhibitor (anti-miR-140) and its control (anti-miR-NC) were synthesized by Hanbio (Shanghai, China). Circ_0000231 (oe-circ) and RAP1B (RAP1B) overexpression constructs, and their control plasmids (oe-NC and pcDNA) were purchased from GenePharma (Shanghai, China). Cell transfection was performed using Lipofectamine 2000 transfection reagent (Invitrogen) when cells reached to 60-80% confluence.

CCK-8 assay

Cell proliferation was measured using CCK-8 assay kit (Beyotime, Nantong, China) as previously reported. Briefly, 2×10^3 cells were seeded in 96-well plates and cultured for 0, 24, 48, 72, and 96 h. To evaluate PTX resistance, cells in 96-well plates were exposed to different doses of PTX. The absorbance values at 450 nm were then measured using an enzyme immunoassay analyzer. IC50 value represented the half-maximum inhibitory concentration of PTX.

Fluorescence in situ hybridization (FISH)

The subcellular location of circ_0000231 and miR-140 was detected by FISH assay using a fluorescent in situ hybridization kit (Servicebio, Wuhan, China) according to the manufacturer's protocol. Nuclei were stained by diamidino-2-phenylindole (DAPI). Images were captured with a confocal microscope (Olympus).

Transwell assay

To determine cell invasion ability, transwell chambers in 24-well plates were used. Briefly, transfected ovarian cells were suspended in serum free medium, and 2×10^5 cells/per well were plated into the upper chamber (Corning, NY, USA), in which the upper surface of the filter was precoated with Matrigel (Solarbio, Beijing,

China), whereas the bottom chamber contained RPMI-1640 complete medium with 10% FBS. After culture for 48 h, the invaded cells were stained and imaged. For transwell migration assay, similar procedure was performed except that the the upper surface of the filter in the upper chamber was not coated with Matrigel.

Flow cytometry

The transfected ovarian cells were washed twice in ice cold PBS and then resuspended in binding buffer. The cells were respectively stained with Annexin V-FITC (BestBio, Shanghai, China) and propidium iodide (PI) for 10 min in a dark room and then analyzed with a flow cytometer (FACScan, BD, USA), and apoptotic fractions were analyzed by FlowJo software.

Western blot

The cell and tissue lysates were prepared with RIPA buffer containing protease inhibitor and phosphatase inhibitor cocktails (Beyotime, Shanghai, China), and the total protein was quantified with a BCA kit (Beyotime, Shanghai, China). Equal amount of protein from each sample was separated by SDS PAGE and blotted onto PVDF membranes (Millipore, Billerica, MA). The membranes incubated with primary antibodies against RAP1B (Proteintech, China), E-cadherin (Proteintech, China), Vimentin (Proteintech, China), MMP9 (Proteintech, China), β-tubulin III (Wanleibio, China), β-actin (Wanleibio, China) at 4°C overnight before incubated with the corresponding secondary antibody (Proteintech, China) for 1 h at room temperature. Enhanced chemiluminescence Western Blotting Substrate (Wanleibio, China) and X-ray films were used to visualize the protein bands.

Immunohistochemical staining (IHC)

Tumor tissues were fixed in 4% paraformaldehyde (PFA) and embedded in paraffin. The paraffin blocks were then sectioned at a thickness of 5 μm, and the tissue sections were attached to a polylysine-coated slide overnight at 60°C and dewaxed. The slides were stained with anti-β-tubulin III (Wanleibio, China) and goat anti-rabbit IgG/HRP antibody (Solarbio, China). The color development was performed by incubation with the corresponding secondary antibody. Finally, the number of β-tubulin III-positive cells was evaluated under an optical microscope.

Luciferase reporter assay

The circ_0000231 (circ_0000231-WT-3'UTR) and RAP1B (RAP1B-WT-3'UTR) promoter sequence containing the miR-140 mimic binding site and the circ_0000231 mutant (circ_0000231-MUT-3'UTR) and RAP1B mutant (RAP1B-MUT-3'UTR) promoter sequence were synthesized and cloned into the psiCHECK vector (Hanbio, Shanghai, China). All these plasmids were co-transfected with miR-NC or miR-140 into cells using Lipofectamine 2000. At 24 h after transfection, the reporter Firefly luciferase and Renilla luciferase activities were measured via Dual-Luciferase Assay Kit (Beyotime, Shanghai, China). The relative firefly luciferase activity was normalized to Renilla luciferase activity which served as transfection control.

RNA-immunoprecipitation (RIP) assay

The interaction between circ_0000231 and miR-140 was assessed by a Magna RIP RNA-Binding Protein Immunoprecipitation Kit (Millipore, MA) according to manufacturer's instruction. Briefly, the cell lysates were incubated with Argonaute 2 (AGO2; Millipore) or control IgG (Millipore) antibody. Then, the immunoprecipitated RNA was extracted and analyzed for the expression of circ_0000231 and miR-140 by qRT-PCR.

Mouse xenograft tumor

Female BALB/c nude mice (about 5 weeks old) were randomly divided into four groups (n=3). Stably transfected 2×10^6 SKOV3-TR30 cells expressing sh-NC or sh-circ_000023 were subcutaneously injected into the right shank of mice. Five days after cell inoculation, the mice were treated with PTX (5 mg/kg) or normal saline via intraperitoneal injection every 3 days. Tumor growth was monitored, and the tumor volume was calculated using the formula: Volume (mm^3) = length × width^2 × 0.5. At day 28, mice were sacrificed, and the xenograft tumors were extracted and weighed. All study protocols involving animals were approved by the Animal Ethics Committee of China Medical University.

Statistical analysis

All data were shown as the mean ± standard deviation from at least three independent

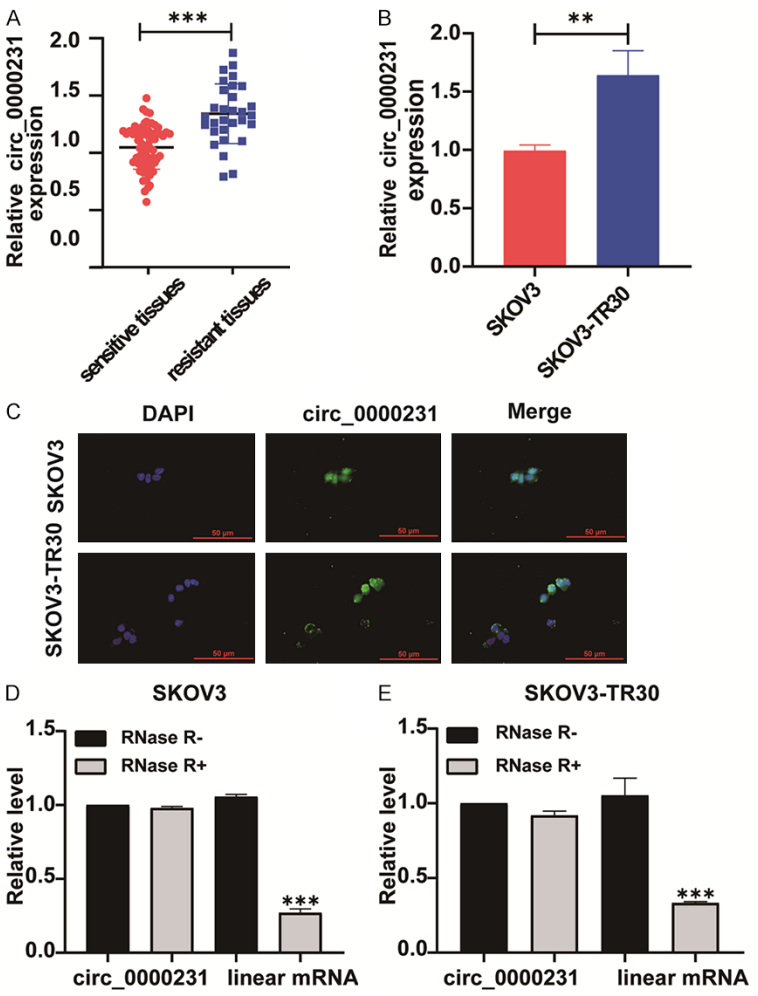

Figuer 1. High expression of circ_0000231 was a risk factor of ovarian cancer. (A) The expression of circ_0000231 was measured in chemosensitive (n=65) and chemoresistant (n=30) OC tissues by qRT-PCR. (B) Circ_0000231 level was measured in chemosensitive SKOV3 and chemoresistant SKOV3-TR30 OC cells by qRT-PCR. (C) FISH was used to determine the subcellular location of circ_0000231 and miR-140 in SKOV3 and SKOV3-TR30 cells (blue: DAPI nuclear staining; green: circ_0000231; red: miR-140). (D, E) qRT-PCR for the expression of circ_0000231 and ARHGAP12 mRNA in SKOV3 (D) and SKOV3-TR30 (E) cells with or without RNase R treatment. Data were expressed as mean ± SD. ***P<0.001.

experiments. Spearman analysis was used to analyze the relationship of associated factors. Statistical analysis was performed using SPSS 26.0. P<0.05 was considered statistically significant.

Results

Circ_0000231 was highly expressed in PTX-resistant OC tissues and cells

We first measured the expression of circ_0000231 in PTX-resistant OC tissues by qRT-PCR and found that the expression of circ_0000231 was significantly higher in the chemoresistant OC tissues (30 cases) than in the chemosensitive group (65 cases) (**Figure 1A**). Similarly, significantly lower expression of circ_0000231 was detected in SKOV3 cells than in SKOV3-TR30 cells (**Figure 1B**). In addition, we examined the subcellular location of Circ_0000231 by FISH analysis, and circ_0000231 was mainly located in the cytoplasm of SKOV3 and SKOV3-TR30 cells (**Figure 1C**). Furthermore, the fragment of linear ARHGAP-12 mRNA could be digested by RNase R, whereas circ_0000231 was not affected by RNase R treatment (**Figure 1D**, **1E**). Moreover, using the median expression level of circ_0000231 as cutoff value, we divided the OC patients into low- and high-expression groups. As shown in **Table 1**, circ_0000231 expression was significantly correlated with FIGO stage.

Circ_0000231 regulated the malignancy and PTX chemosensitivity of OC cells in vitro

Next, we investigated the effect of circ_0000231 on the sensitivity of OC cells to paclitaxel by using circ_0000231 knockdown or overexpression approaches. circ_0000231 knockdown was achieved by transfecting si-NC into SKOV3-TR30 cells (**Figure 2A**), while circ_0000231 overexpression was achieved by transfecting oe-circ construct into SKOV3 cells (**Figure 2B**). CCK-8 assays showed that si-circ inhibited the proliferation of SKOV3-TR30 cells (**Figure 2C**, **2D**). In addition, we determined the IC50 of PTX in SKOV3 and SKOV3-TR30 cells by CCK-8 assays (**Figure 2E**, **2F**). Furthermore, silencing of circ_0000231 markedly enhanced the apoptosis of OC cells (**Figure 2G**). Conversely, the

Table 1. Association of circ_0000231 expression with clinicopathological features of OC patients

Characteristics	N	Low	High	*P*-value	χ^2 value
Age (years)				*P=0.630*	χ^2=0.232
<50	35	25	10		
≥50	60	40	20		
FIGO				*P=0.000*	χ^2=13.565
I-II	27	26	1		
III-IV	68	39	29		
Differeciation				*P=0.576*	χ^2=0.312
High	32	10	6		
Low	63	55	24		
Positive lymph node				*P=0.113*	χ^2=2.519
No	43	33	10		
Yes	52	32	20		

apoptosis of OC cells was inhibited by the overexpression of circ_0000231 (**Figure 2H**). Moreover, transwell assays demonstrated that Circ_0000231 knockdown significantly inhibited, while Circ_0000231 overexpression promoted the invasion and migration of SKOV3-TR30 cells (**Figure 2I**, **2J**). At molecular level, we found that circ_0000231 knockdown attenuated the expression of EMT marker proteins in SKOV3. Consistently, overexpression of circ_0000231 significantly increased the levels of EMT marker proteins (**Figure 2K**). Collectively, these results suggest that circ_0000231 regulated PTX-resistance and the malignancy of OC cells.

MiR-140 was a direct target of circ_0000231

To understand the functional mechanism of circ_0000231, we used two prediction websites (circBank and circinteractome) to predict the potential target miRNAs that might bind to circ_0000231 (**Figure 3A**). qRT-PCR detected the expression of four possible miRNAs (miR-558, miR-622, miR-140 and miR-135b-5p) in SKOV3-TR30 cells transfected with either si-NC or si-circ. We found that the expression of miR-140 was dramatically upregulated in circ_0000231 knockdown cells (**Figure 3B**); hence, we focused our study on miR-140. Potential binding sites between circ_0000231 and miR-140 were predicted by CircInteractome (**Figure 3C**). To explore the effect of altered miR-140 expression on circ_0000231, we used qRT-PCR to examine the expression of circ_0000231 in cells transfected with either anti-miR-140 or miR-140 and found that the expression of circ_0000231 was regulated by miR-140 (**Figure 3D**). To confirm that miR-140 was the target of circ_0000231, we used dual-luciferase reporter assay and RIP assay and found that miR-140 could bind to circ_0000231 (**Figure 3E**, **3F**). FISH assay suggested that miR-140 and circ_0000231 were mainly co-localized in the cytoplasm (**Figure 3G**). Moreover, we found the expression of miR-140 was decreased in PTX-resistant OC tissues and cells (**Figure 3H**, **3I**). Importantly, we observed a significant inverse association between miR-140 and circ_0000231 expression in OC samples (**Figure 3J**). Together, these results supported that miR-140 was a target gene of circ-0000231 in OC cells, and circ-0000231 negatively regulated the expression of miR-140.

MiR-140 regulated the malignancy and PTX chemosensitivity of OC cells

We determined the role of miR-140 in OC cells by manipulating its expression. The overexpression or knockdown of miR-140 was confirmed by qRT-PCR (**Figure 4A**, **4B**). We found that miR-140 regulated cells proliferation (**Figure 4C**, **4D**). The IC50 assessment assays showed that miR-140 suppressed the PTX chemosensitivity of OC cells (**Figure 4E**, **4F**). Flow cytometry revealed an increased apoptosis in miR-140 mimic-expressing SKOV3-TR30 cells compared with NC-expressing SKOV3-TR30 cells, and miR-140 suppression could significantly decrease the apoptosis of SKOV3-TR30 cells (**Figure 4G**). The transwell assays indicated that the miR-140 inhibitor-treated cells had a markedly increased migration and invasion ability compared with the control cells (**Figure 4H**). Conversely, the miR-140 mimic expression decreased the migration and invasion of OC cells (**Figure 4I**). Furthermore, miR-140 inhibitor significantly reduced the protein levels of vimentin, β-tubulin-III and MMP9, while significantly increased the protein level of E-cadherin. Consistently, overexpression of miR-140 upregulated the protein levels of vimentin, β-tubulin-III and MMP9, while downregulated the protein level of E-cadherin (**Figure 4J**). Taken together, these results suggested that miR-140 knockdown inhibited PTX resistance and the malig-

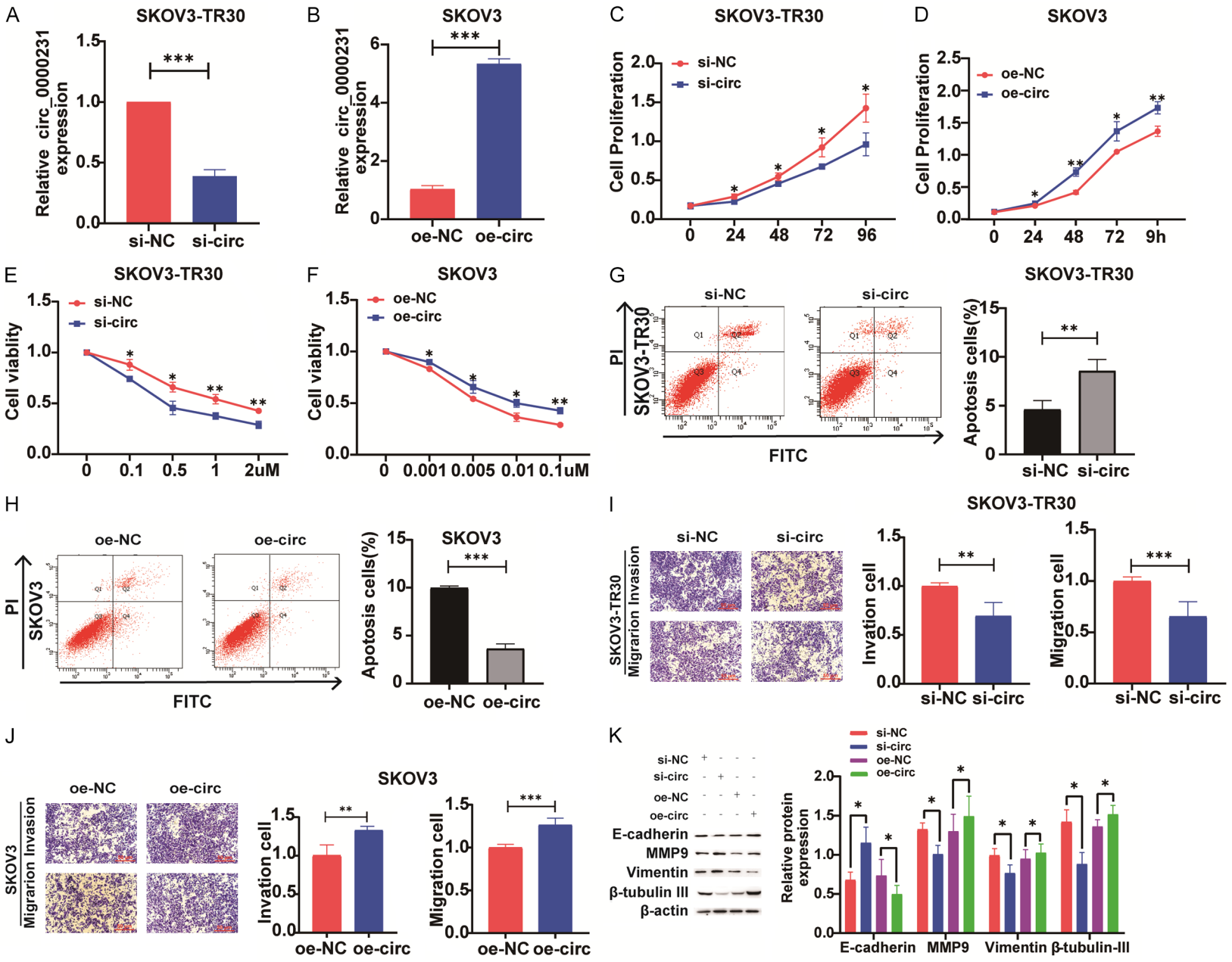
A
SKOV3-TR30
Relative circ_0000231 expression
si-NC
si-circ
B
SKOV3
Relative circ_0000231 expression
oe-NC
oe-circ
C
SKOV3-TR30
Cell Proliferation
si-NC
si-circ
D
SKOV3
Cell Proliferation
oe-NC
oe-circ
E
SKOV3-TR30
Cell viablity
F
SKOV3
Cell viablity
G
SKOV3-TR30
PI
FITC
Apotosis cells(%)
H
SKOV3
I
SKOV3-TR30
Migrarion Invasion
Invation cell
Migration cell
J
SKOV3
K
E-cadherin
MMP9
Vimentin
β-tubulin III
β-actin
Relative protein expression

Figure 2. Circ_0000231 promoted the proliferation, apoptosis, metastasis, and chemoresistance of ovarian cancer cell. A, B. The transefection efficiency of circ_0000231 in OC cells was determined by qRT-PCR. C, D. CCK-8 assays were performed to determine the proliferation of OC cells expressing si-circ or oe-circ. E, F. The sensitivity of OC cells and chemoresistant OC cells to PTX was assessed by CCK-8 assays. G, H. Flow cytometry was carried out to detect the proportion of apoptotic cells. I, J. Cell migration and invasion capacities were determined by transwell assays (magnification: 100×). K. Inhibition of circ_0000231 led to an increased expression of the epithelial cell marker E-cadherin and a decreased expression of mesenchymal cell marker vimentin as well as the related proteins MMP9 and β-tubulin III. Overexpression of circ_0000231 led to an opposite expression pattern. Data were expressed as mean ± SD. $^{*}P<0.05$, $^{**}P<0.01$, $^{***}P<0.001$.

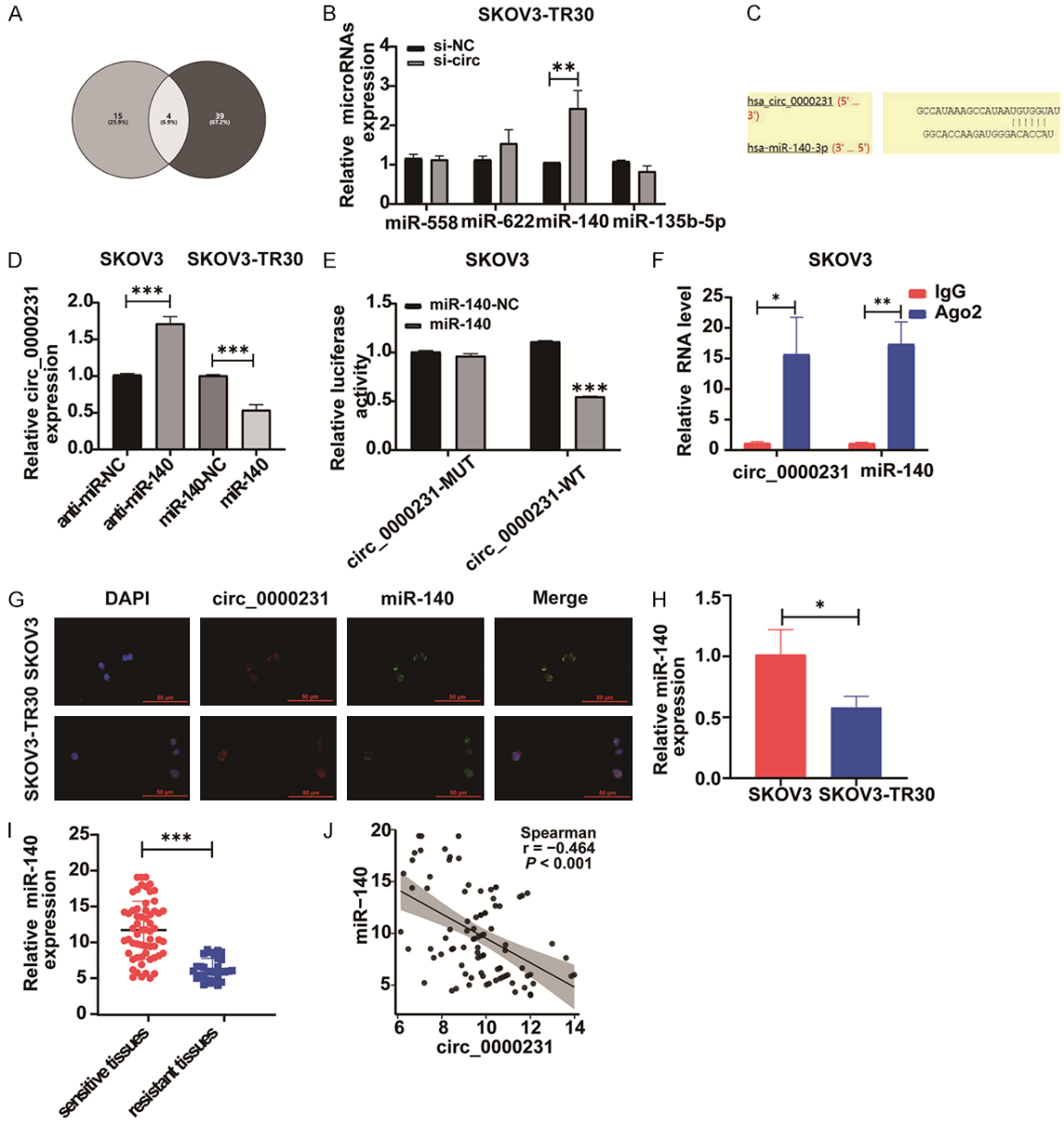

Figure 3. Circ_0000231 acted as a miR-140 sponge. A. Two websites (circBank and circinteractome) were used to predict potential miRNAs that might bind to circ_0000231. B. The effect of circ_0000231 knockdown by si-circ_0000231 transfection on the expression of four possible miRNA targets (miR-558, miR-622, miR-140 and miR-135b-5p). C. The putative binding site between circ_0000231 and miR-140 was depicted by circinteractome. D. qRT-PCR was applied to examine the expression of circ_0000231 in cell expressing miR-140 inhibitor or miR-140 mimic. E. Dual-luciferase reporter assay was conducted to verify the target relationship between circ_0000231 and miR-140. F. The RIP assay indicated the direct interaction between circ_0000231 and miR-140. G. FISH was

performed to determine the subcellular location of circ_0000231 and miR-140. H. qRT-PCR was applied to detect the expression of miR-140 in SKOV3 and SKOV3-TR30 cells. I. The expression of miR-140 was detected in chemosensitive and chemoresistant OC tissues by qRT-PCR. J. The correlation between the expression of miR-140 and circ_0000231 was assessed using Spearman's correlation coefficient.

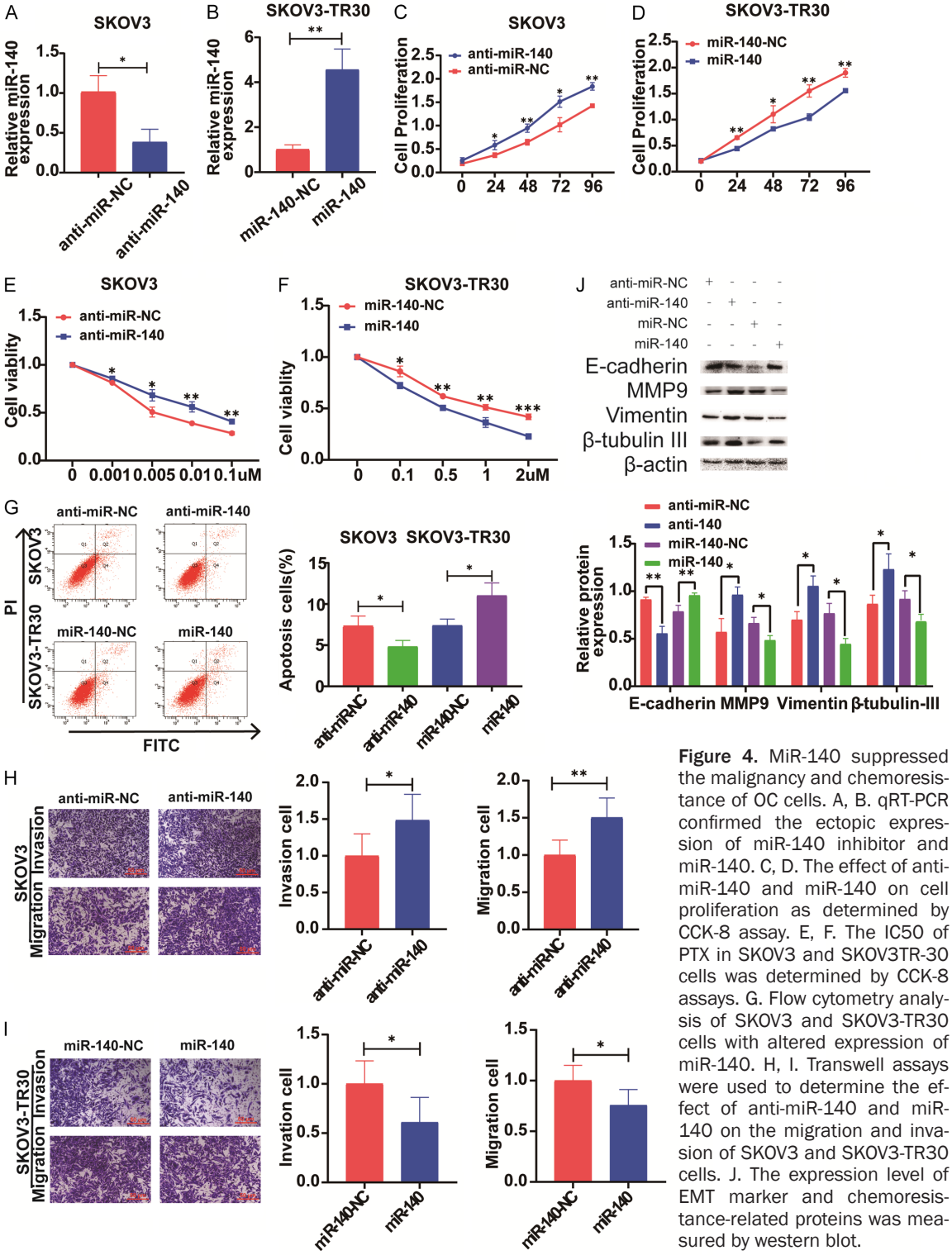

Figure 4. MiR-140 suppressed the malignancy and chemoresistance of OC cells. A, B. qRT-PCR confirmed the ectopic expression of miR-140 inhibitor and miR-140. C, D. The effect of anti-miR-140 and miR-140 on cell proliferation as determined by CCK-8 assay. E, F. The IC50 of PTX in SKOV3 and SKOV3TR-30 cells was determined by CCK-8 assays. G. Flow cytometry analysis of SKOV3 and SKOV3-TR30 cells with altered expression of miR-140. H, I. Transwell assays were used to determine the effect of anti-miR-140 and miR-140 on the migration and invasion of SKOV3 and SKOV3-TR30 cells. J. The expression level of EMT marker and chemoresistance-related proteins was measured by western blot.

nancy of OC cells, whereas overexpression of miR-140 exerted an opposite effect.

Inhibition of miR-140 reversed the effect of circ_0000231 knockdown on the progression and PTX resistance of OC cells

We further explored the functional relationship between MiR-140 and circ_0000231. We first confirmed that MiR-140 inhibition could reverse the circ_0000231 knockdown-induced upregulation of miR-140 in SKOV3-TR30 cells. Then, we performed CCK-8 assays and found that miR-140 inhibition could markedly rescue circ_0000231 silence-mediated suppression on the proliferation of OC cells (**Figure 5A**). Moreover, the IC50 of PTX analysis showed that miR-140 inhibition clearly reversed circ_0000231 knockdown-induced chemosensitivity in SKOV3-TR30 (**Figure 5B**). The inhibition of miR-140 also attenuated the effect of circ_0000231 upregulation on the apoptosis of OC cells (**Figure 5C**). Consistently, miR-140 suppression could reverse the inhibitory effect of circ_0000231 depletion on cell migration and invasion (**Figure 5D**). The expression of vimentin, β-tubulin-III and MMP9 in si-NC- and anti-miR-140-expressing cells were upregulated, while the expression of E-cadherin was reduced (**Figure 5E**). Together, these results suggested that miR-140 silencing could attenuated the tumor-suppressing effect of circ_0000231 silencing.

Circ_0000231 miR-140 positively regulated the expression of RAP1B in PTX-resistant OC cells

Using TargetScan, we predicted that RAP1B might be the target gene of miR-140. RAP1B expression was dramatically declined in SKOV3-TR30 cells transfected with si-circ or miR-140 mimic and increased in SKOV3 cells transfected with oe-circ (Supplementary Materials). The TargetScan analysis showed that RAP1B possessed sites complementary to miR-140 on its 3'UTR (**Figure 6A**). Then, we constructed luciferase reporter vectors containing the wild-type or mutant sequence of miR-140 MREs and co-transfected them with RAP1B. The luciferase assay confirmed that miR-140 targeted RAP1B and negatively regulated RAP1B expression (**Figure 6B**). RAP1B level was higher in SKOV3-TR30 cells than in SKOV3 cells (**Figure 6C**). In addition, the expression of RAP1B was obviously increased in PTX-resistant OC tissues (**Figure 6D**). Western blot analysis also showed the same results (Supplementary Materials). Importantly, we performed Spearman analysis to reveal the relationship between RAP1B and miR-140. The results showed that RAP1B level was negatively correlated with miR-140 (**Figure 6E**). Furthermore, western blot analysis showed that RAP1B expression was decreased in si-circ-expressing cells but increased in oe-circ-expressing cells (**Figure 6F**), supporting the conclusion from bioinformatics analysis. Consistently, RAP1B expression was increased in anti-miR-140-expressing cells and decreased in miR-140 (**Figure 6G**). We further explore the effect of RAP1B on the PTX resistance of OC cells by RAP1B overexpression experiments (Supplementary Materials). We found that RAP1B overexpression not only significantly increased the proliferation of SKOV3-TR30 (**Figure 6H**) but also promoted PTX resistance with elevated IC50 value (**Figure 6I**). Importantly, overexpression of RAP1B reversed circ_0000231 knockdown-induced effect in proliferation, apoptosis, invasion, migration, PTX resistance, and the expression of related proteins (**Figure 6J-O**). Hence, we concluded that circ_0000231 positively regulated RAP1B expression by sponging miR-140.

Circ_0000231 knockdown enhanced PTX sensitivity of OC cells in vivo

The xenograft tumor model was used to assess the effect of circ_0000231 on the growth and chemoresistance of OC in vivo. Sh-NC- or sh-circ-0000231-expressing OC cells were subcutaneously injected into the mice. Mice were randomized into four groups: sh-circ_0000231 + PTX, sh-circ_0000231 + normal saline (NS), sh-NC + PTX, and sh-NC + NS. As shown in **Figure 7A**, comparing the tumor growth among these four groups, maximum tumor volume was observed in sh-NC+ NS group. The tumor volume was significantly decreased in sh-circ_0000231 + PTX mice (**Figure 7B**). When comparing tumor weight, the smallest tumor was also observed in this sh-circ_0000231 + PTX group (**Figure 7C**), confirming that the inhibition of circ_0000231 affected the growth of PTX-resistant OC cells. Furthermore, IHC assays showed that the tumors derived from sh-circ_0000231-expressing cells displayed a decreased percentage of β-tubulin III-positive cells (**Figure 7D**). Collec-

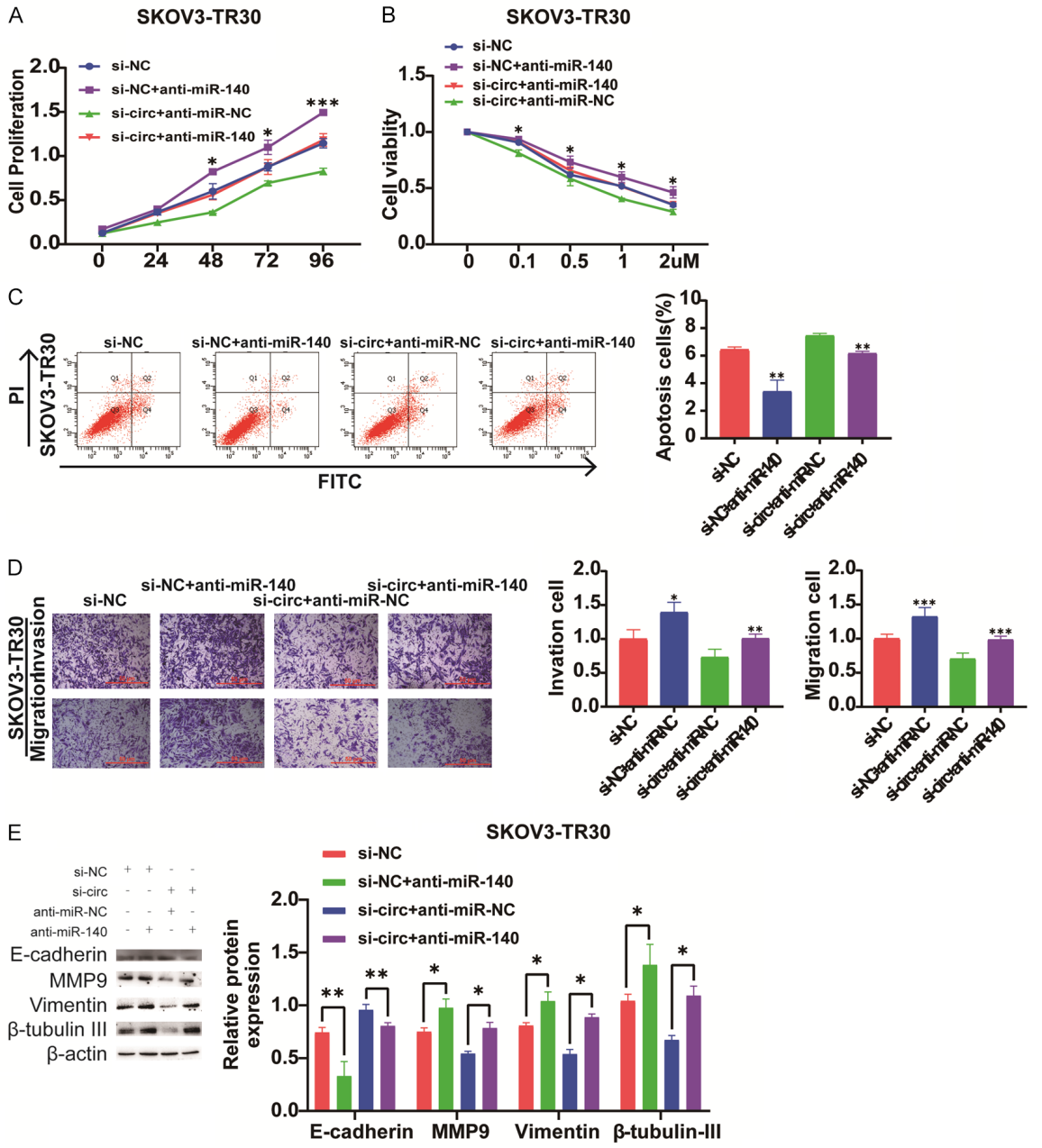

Figure 5. Inhibition of miR-140 reversed the effect of circ_0000231 knockdown on the progression and PTX resistance of OC cells. A. CCK-8 assay was performed to evaluate the effect of circ_0000231 and miR-140 on the proliferation of SKOVE-TR30 cells. B. The IC50 of PTX on SKOV3TR-30 cells was determined by CCK-8 assays. C. The effect of miR-140 and circ_0000231 on apoptosis was analyzed using flow cytometry. D. The effect of miR-140 and circ_0000231 on cell migration and invasion was assessed by transwell assays. E. The levels of EMT markers and resistance-related proteins were determined by western blot.

tively, the combination of circ_0000231 knockdown and PTX treatment resulted in the synergistic inhibition of OC cell growth in vivo.

Discussion

Chemotherapy is widely used for OC treatment nowadays; however, the main obstacle to successful chemotherapy is the development of chemoresistance [11]. In this study, we explored the involvement of circRNA in paclitaxel resistance in OC and demonstrated that circ_0000231 was upregulated in PTX-resistant OC cell lines and tissues.

The effects of circ_0000231 in paclitaxel resistance were assessed in vitro by overexpression and silencing experiments. The suppression of

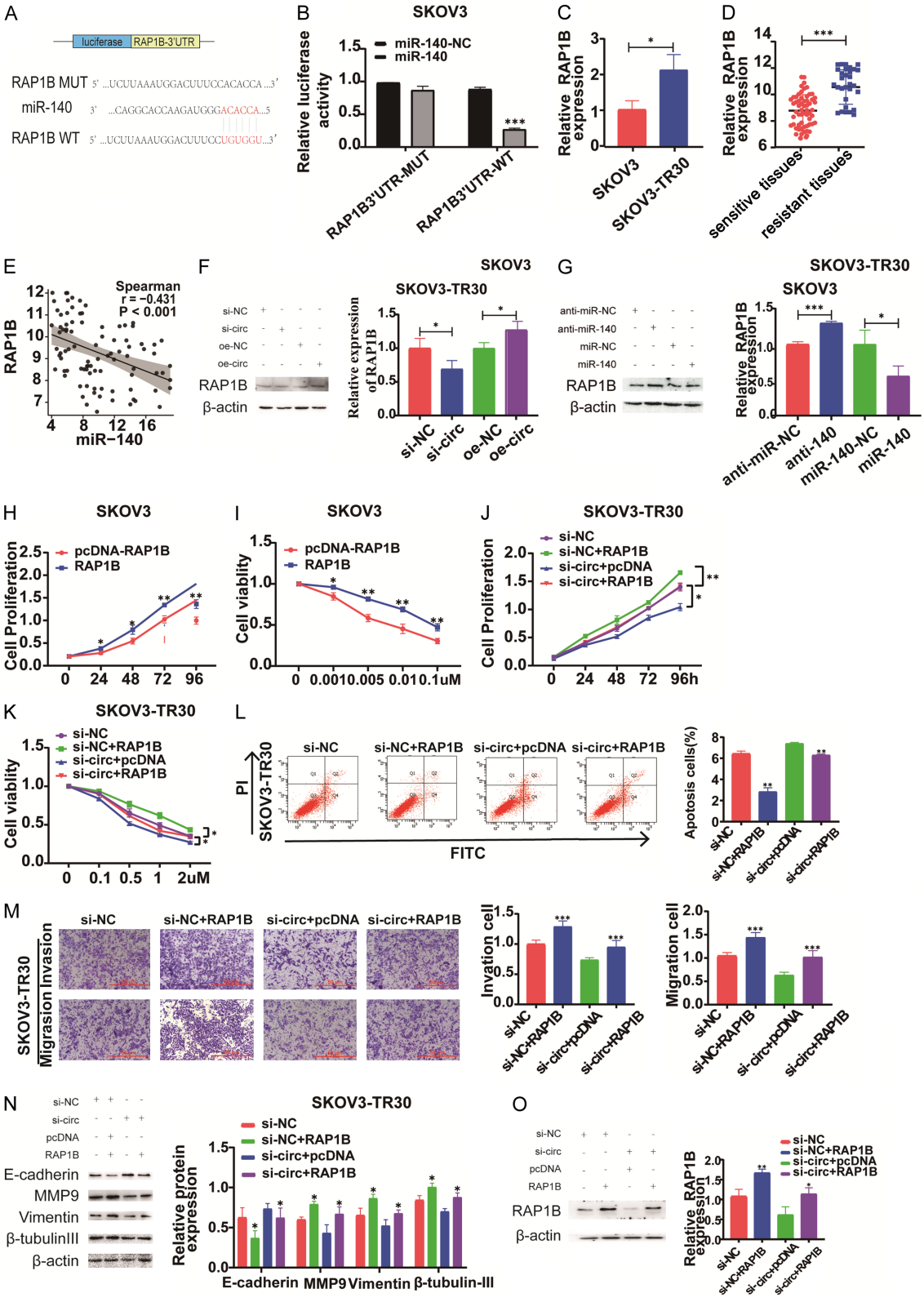

Figure 6. Circ_0000231 Positively regulated RAP1B expression by interacting with miR-140 in PTX-Resistant OC Cells. A. The complementary sites between RAP1B and miR-140 were predicted by Targetscan database. B. Luciferase reporter assay demonstrated that miR-140 mimic significantly decreased the luciferase activity of RAP1B-WT in SKOV3 cells. C. The expression of RAP1B was measured by qRT-PCR in SKOV3 and SKOV3-TR30 cells. D. The ex-

pression of RAP1B was measured by qRT-PCR in OC-resistant and OC-sensitive tissues. E. The correlation between the expression of miR-140 and RAP1B was assessed using Spearman's correlation coefficient. F. The expression of RAP1B was measured by western blot in si-circ- and oe-circ-expressing cells. G. The expression of RAP1B was measured by western blot in anti-miR-140- and miR-140-expressing cells. H. CCK-8 assay was performed to evaluate the effect of increased RAP1B on the proliferation of SKOVE-TR30 cells. I. IC50 was determined by CCK-8 assays in SKOV3TR-30 cells that were treated with different concentrations of PTX. J. The proliferation of SKOV3-TR30 was evaluated by CCK8 assay. K. IC50 was determined by CCK-8 assays in SKOV3TR-30 cells that were treated with different concentrations of PTX. L. The apoptosis of co-transfected cells was analyzed using flow cytometry. M. Cell invasion was measured by transwell assays. N. The levels of EMT markers and resistance-related proteins were measured by western blot. O. The expression of RAP1B was measured by western blot in transfected SKOV3-TR30 cells.

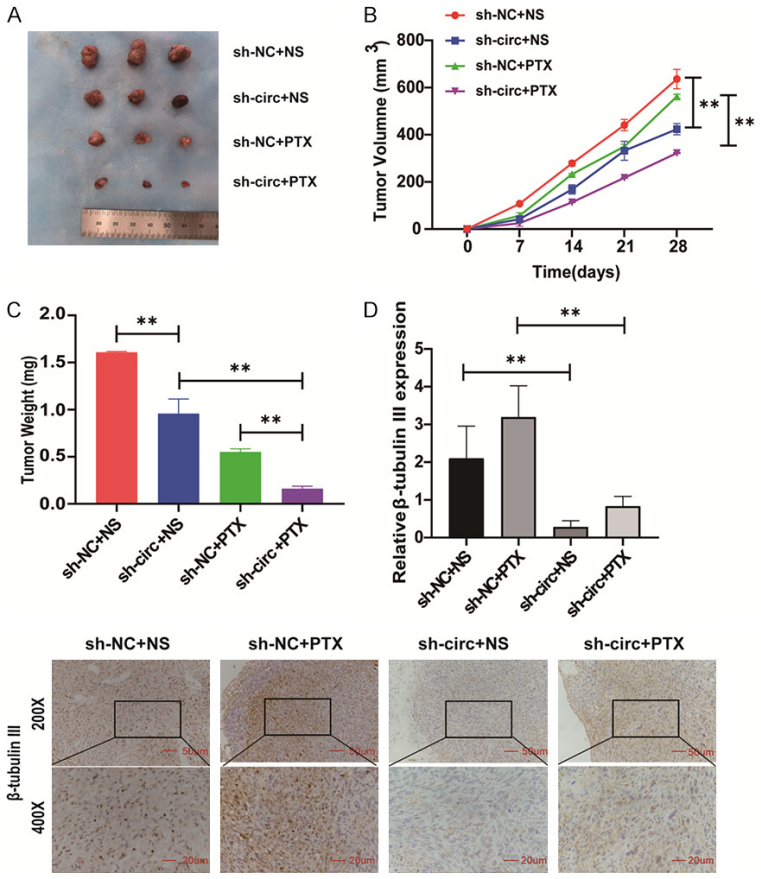

Figure 7. The growth of mouse xenograft tumor. A. Mouse xenograft tumor. B. The tumor size was measured every 7 d, and the tumor was resected 28 days after cell inoculation. C. The tumor weight in different groups was examined at day 28 post inoculation. D. The expression of β-tubulin III in xenograft tumors was examined by IHC. Original magnification: 200×, 400×.

circ_0000231 promoted paclitaxel sensitivity and apoptosis but inhibited cell proliferation, migration, and invasion, whereas overexpression of circ_0000231 had the opposite effect, indicating the role of circ_0000231 on the malignancy and PTX resistance of ovarian cancer, Importantly, the same result was also demonstrated in vivo. These results also suggested that circ_0000231 could serve as a potential diagnostic and therapeutic target in OC. To explore the molecular mechanism underlying the regulatory role of circ_0000231, we carried out a series of biochemical studies and found that circ_0000231 was mainly located in the cytoplasm of SKOV3 cells, suggesting that circ_0000231 might regulate gene expression at post-transcriptional level. In other diseases, circ_0000231 has been reported to act as miRNA "sponge" affecting miRNA activity. Liu [12] et al. found that circ_0000231 knockdown inhibited the progression and glycolysis of colorectal cancer cells by downregulating MYO6 expression through sponging miR-502-5p. Circ_0000231 was also reported to promote atherosclerosis progression through miR-1236-3p/HOXB7 regulatory axis [13]. Thus, we speculated that circ_0000231 might exert its role in PTX-resistant OC through regulating the miRNA/mRNA axis.

MiR-140 has been reported to regulate cell proliferation, apoptosis, migration and invasion in various cancers [14], such as breast cancer [15], esophageal squamous cell carcinoma [16], lung cancer [17], and OC [18]. Qiao et al. found that miR-140 was sponged by LINC00852 and involved in LINC000852-mediated OC progression [19]. MiR-140 also inhibits ovarian cancer growth by repression of PDGFRA [18]. In our study, the bioinformatics analysis and luciferase reporter assay showed that circ_0000231 competitively bound to miR-

140. miR-140 was downregulated in PTX-resistant OC tissues and cells. In addition, miR-140 acts as a tumor suppressor to inhibit the proliferation, migration, invasion, and drug resistance of PTX-resistant OC cells. Decreased expression of miR-140 promoted the proliferation, migration, invasion, and PTX resistance of OC cells. We further investigated whether circ_0000231 exerted PTX resistance of OC cells through regulating miR-140 by circ_0000231 and miR-140 co-transfection experiments in SKOV3-TR30 cells. We determined that MiR-140 inhibitor reversed the tumor suppressive effects induced by the silencing of circ_0000231.

We also predicted the target gene of miR-140 by using TargetScan database and identified PAP1B as a potential target gene, which was further confirmed by dual-luciferase reporter assay. Ras-related protein 1 (Rap1) is a ubiquitously expressed small GTPase and has two isoforms: RAP1A and RAP1B [20]. In recent years, an increasing number of studies have found that RAP1B regulates the occurrence and development of tumors [21]. RAP1B, as an oncogene, has been reported to be overexpressed in OC cells [22], consistent with the findings in our study. We also found that RAP1B knockdown could inhibit the migration and invasion of OC cells. Moreover, we found that RAP1B expression was higher in PTX-resistant than in PTX-sensitive OC tissues and cells. Overexpression of RAP1B could promoted the proliferation of PTX-resistant cells. Importantly, inhibition of circ_0000231-mediated suppression of RAP1B protein expression was significantly recuperated by miR-140 inhibitors. Rescue experiments further confirmed that RAP1B overexpression abrogated the suppressive effect of circ_0000231 knockdown. Taken together, we were the first to demonstrate the involvement of circ_0000231/miR-140/RAP1B regulatory axis in OC development and chemoresistance, which highlighted their role as promising therapeutic target in OC treatment.

Nevertheless, our study had some limitations. First, only a limited number of ovarian cancer lines were used in this study, which needs to be expanded to more cell lines to make our conclusion more convincing. Second, it will be significant to determine the role of circ_0000231 in other cancer types to reveal if the function of circ_0000231 is OC specific or can be generalized to other cancer types. Lastly, other mechanisms besides circ_0000231 are very likely to involve in the regulation of OC progression and chemoresistance, which needs further exploration.

In summary, circ_0000231 was overexpressed in PTX-resistant OC cells and tissues. Circ_0000231 might act as sponge for anti-oncogenic miR-140 to upregulate RAP1B and promote the PTX resistance and progression of OC. In addition, circ_0000231 also enhanced the expression of EMT marker proteins in PTX-resistant cells. We were the first to demonstrate the involvement of circ_0000231/miR-140/RAP1B axis in PTX-resistant OC cells. Therefore, our findings provided the rationale for targeting circ_0000231/miR-140/RAP1B axis in the treatment of chemoresistant OC.

Acknowledgements

Funding Natural Science Foundation of Liaoning Province (Grant No. 201800832); The Outstanding Scientific Fund of Shengjing Hospital (Grant No. 201705).

Disclosure of conflict of interest

None.

Address correspondence to: Min Wang, Department of Obstetrics and Gynecology, Shengjing Hospital of China Medical University, Shenyang, Liaoning, China. Tel: +86-18940251222; E-mail: wm21st@126.com

References

[1] Miller KD, Fidler-Benaoudia M, Keegan TH, Hipp HS, Jemal A and Siegel RL. Cancer statistics for adolescents and young adults, 2020. CA Cancer J Clin 2020; 70: 443-459.

[2] Modok S, Mellor HR and Callaghan R. Modulation of multidrug resistance efflux pump activity to overcome chemoresistance in cancer. Curr Opin Pharmacol 2006; 6: 350-354.

[3] Salmena L, Poliseno L, Tay Y, Kats L and Pandolfi P. A ceRNA hypothesis: the Rosetta stone of a hidden RNA language? Cell 2011; 146: 353-358.

[4] Zhang S, Zhu D, Li H, Li H, Feng C and Zhang W. Characterization of circRNA-associated-ceRNA networks in a senescence-accelerated mouse prone 8 brain. Mol Ther 2017; 25: 2053-2061.

[5] Fontemaggi G, Turco C, Esposito G and Di Agostino S. New molecular mechanisms and clinical impact of circRNAs in human cancer. Cancers (Basel) 2021; 13: 3154.
[6] Cui X, Wang J, Guo Z, Li M, Li M, Liu S, Liu H, Li W, Yin X, Tao J and Xu W. Emerging function and potential diagnostic value of circular RNAs in cancer. Mol Cancer 2018; 17: 123.
[7] Zhao Z, Ji M, Wang Q, He N and Li Y. Circular RNA Cdr1as upregulates SCAI to suppress cisplatin resistance in ovarian cancer via miR-1270 suppression. Mol Ther Nucleic Acids 2019; 18: 24-33.
[8] Zhang S, Cheng J, Quan C, Wen H, Feng Z, Hu Q, Zhu J, Huang Y and Wu X. CircCELSR1 (hsa_circ_0063809) contributes to paclitaxel resistance of ovarian cancer cells by regulating FOXR2 expression via miR-1252. Mol Ther Nucleic Acids 2020; 19: 718-730.
[9] Wang J, Li S, Zhang G and Han H. Sevoflurane inhibits malignant progression of colorectal cancer via hsa_circ_0000231-mediated miR-622. J Biol Res (Thessalon) 2021; 28: 14.
[10] Wang Z, Ting Z, Li Y, Chen G, Lu Y and Hao X. MicroRNA-199a is able to reverse cisplatin resistance in human ovarian cancer cells through the inhibition of mammalian target of rapamycin. Oncol Lett 2013; 6: 789-794.
[11] Liu Y, Li H, Ye X, Ji A, Fu X, Wu H and Zeng X. Hsa_circ_0000231 knockdown inhibits the glycolysis and progression of colorectal cancer cells by regulating miR-502-5p/MYO6 axis. World J Surg Oncol 2020; 18: 255.
[12] Shao X, Liu Z, Liu S, Lin N and Deng Y. Astragaloside IV alleviates atherosclerosis through targeting circ_0000231/miR-135a-5p/CLIC4 axis in AS cell model in vitro. Mol Cell Biochem 2021; 476: 1783-1795.
[13] Ghafouri-Fard S, Bahroudi Z, Shoorei H, Abak A, Ahin M and Taheri M. MicroRNA-140: a miRNA with diverse roles in human diseases. Biomed Pharmacother 2021; 135: 111256.
[14] Salem O, Erdem N, Jung J, Münstermann E, Wörner A, Wilhelm H, Wiemann S and Körner C. The highly expressed 5'isomiR of hsa-miR-140-3p contributes to the tumor-suppressive effects of miR-140 by reducing breast cancer proliferation and migration. BMC Genomics 2016; 17: 566.
[15] Chen X, Jiang J, Zhao Y, Wang X, Zhang C, Zhuan L, Zhang D and Zheng Y. Circular RNA circNTRK2 facilitates the progression of esophageal squamous cell carcinoma through upregulating NRIP1 expression via miR-140-3p. J Exp Clin Cancer Res 2020; 39: 133.
[16] Huang H, Wang Y, Li Q, Fei X, Ma H and Hu R. MiR-140-3p functions as a tumor suppressor in squamous cell lung cancer by regulating BRD9. Cancer Lett 2019; 446: 81-89.
[17] Lan H, Chen W, He G and Yang S. MiR-140-5p inhibits ovarian cancer growth partially by repression of PDGFRA. Biomed Pharmacother 2015; 75: 117-122.
[18] Qiao ZW, Jiang Y, Wang L, Wang L, Jiang J, Zhang JR and Mu P. LINC00852 promotes the proliferation and invasion of ovarian cancer cells by competitively binding with miR-140-3p to regulate AGTR1 expression. BMC Cancer 2021; 21: 1004.
[19] Li J, Li Y, Wang S, Che H, Wu J and Ren Y. MiR-101-3p/Rap1b signal pathway plays a key role in osteoclast differentiation after treatment with bisphosphonates. BMB Rep 2019; 52: 572-576.
[20] Tang Z, Peng H, Chen J, Liu Y, Yan S, Yu G, Chen Q, Tang H and Liu S. Rap1b enhances the invasion and migration of hepatocellular carcinoma cells by up-regulating Twist 1. Exp Cell Res 2018; 367: 56-64.
[21] Fan M, et al. MicroRNA-30b-5p functions as a metastasis suppressor in colorectal cancer by targeting Rap1b. Cancer Letters 2020; 477: 144-156.
[22] Lin K, Yeh Y, Chuang C, Yang S, Chang J, Sun S, Wang Y, Chao K and Wang L. Glucocorticoids mediate induction of microRNA-708 to suppress ovarian cancer metastasis through targeting Rap1B. Nat Commun 2015; 6: 5917.

Supplementary Materials

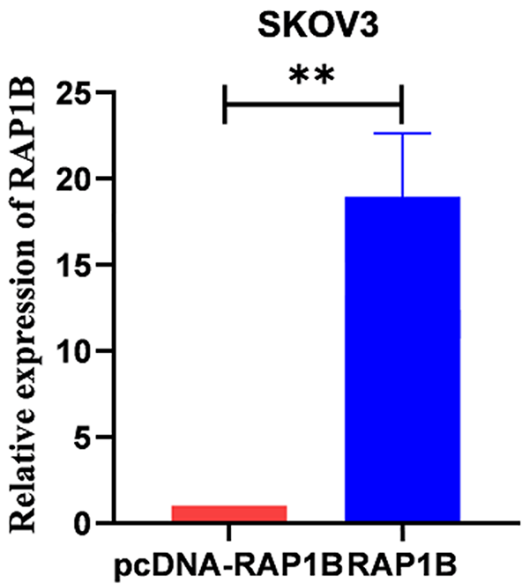

Supplementary Figure 1. rap+.

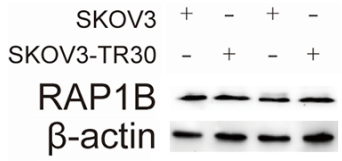

Supplementary Figure 2. RAP-CELL.

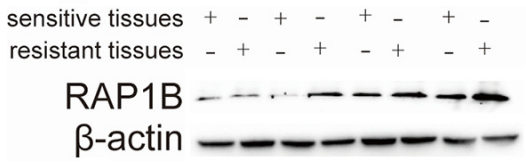

Supplementary Figure 3. RAP-tissue.

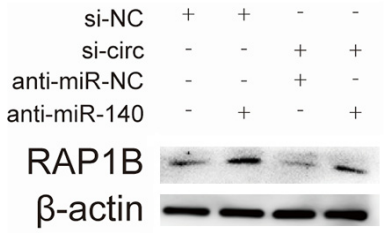

Supplementary Figure 4. si-140-RAP.

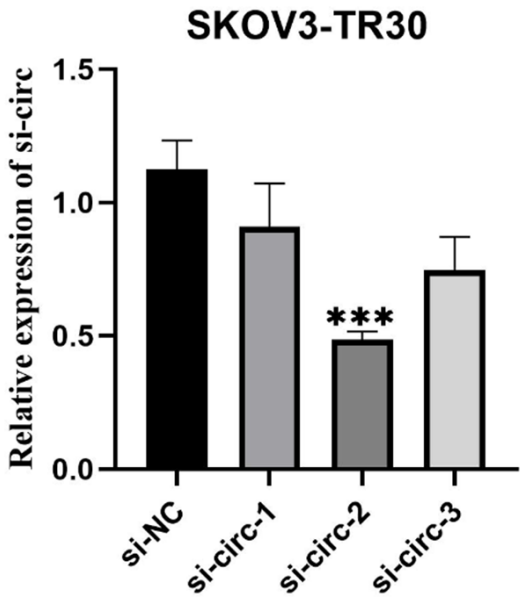

Supplementary Figure 5. si-circ.

Supplementary Table 1. Primer

Circ_0000231	Forward	5'-CCGGTCCAGAGTTCTTGGATG-3'
	Reverse	5'-GCTTAGAACAAGGAGATCTACACCA-3'
β-actin	Forward	5'-CTCCATCCTGGCCTCGCTGT-3'
	Reverse	5'-GCTGTCACCTTCACCGTTCC-3'
miR-140	Forward	5'-CTACCACAGGGTAGAACCACGG-3'
	Reverse	5'-TTTCAGTTATCAATCTGTCACA-3'
U6	Forward	5'-CTCGCTTCGGCAGCACA-3'
	Reverse	5'-AACGCTTCACGAATTTGCGT-3'
RAP1B	Forward	5'-TCAGGAGGCGTTGGAAAGTC-3'
	Reverse	5'-GTGGACTGTGCTGTGATGGA-3'
ARHGAP12	Forward	5'-TCTTCAGAGATCAACAGAAA-3'
	Reverse	5'-AACTTTCCGTTATTATGGGT-3'

Supplementary Table 2. FISH probe

Circ_0000231	green-labeled: 5'-CAGTATCACATTTAAACCCTTATCTGTTCAGTGGA-3'
miR-140	red-labeled, 5'-CTACCATAGGGTAAAACCACTG-3'